

BridgePure: Revealing the Fragility of Black-box Data Protection

Yihan Wang^{*,1,2}, Yiwei Lu^{*,3,4}, Xiao-Shan Gao^{†,‡,1,2}, Gautam Kamath^{†,3,4}, and Yaoliang Yu^{†,3,4}

¹Academy of Mathematics and Systems Science, Chinese Academy of Sciences

²University of Chinese Academy of Sciences

³University of Waterloo

⁴Vector Institute

Abstract

Availability attacks, or unlearnable examples, are defensive techniques that allow data owners to modify their datasets in ways that prevent unauthorized machine learning models from learning effectively while maintaining the data’s intended functionality. It has led to the release of popular black-box tools for users to upload personal data and receive protected counterparts. In this work, we show such black-box protections can be *substantially bypassed* if a small set of unprotected in-distribution data is available. Specifically, an adversary can (1) easily acquire (unprotected, protected) pairs by querying the black-box protections with the unprotected dataset; and (2) train a diffusion bridge model to build a mapping. This mapping, termed *BridgePure*, can effectively remove the protection from any previously unseen data within the same distribution. Under this threat model, our method demonstrates superior purification performance on classification and style mimicry tasks, exposing critical vulnerabilities in black-box data protection.

1 Introduction

The widespread adoption of machine learning (ML) models has raised significant concerns about data privacy, copyright, and unauthorized use of personal information. Specifically, machine learning developers usually rely on crawling web data to create their training sets, which can result in data being trained on without consent of the owners. This has significant potential for misuse. For example, trained models may be used in sensitive applications such as facial recognition (Hill, 2023), resulting in individual re-identification or serious privacy breaches. Another example is training on copyrighted images created by artists. The downstream models could be used for style mimicry, and potentially even direct copyright infringement in cases where training data is exactly replicated by a generative model.

Such unauthorized data use has served as an impetus for broad pushback against the use of ML models. As one particular demographic, artists have been searching for solutions that prevent non-consensual use of their artwork for training ML models. Their desires are somewhat at odds with each other: they would like their artwork to have low value in training an ML model, while simultaneously ensuring that the artwork is high fidelity to preserve the quality of their original work. This has given rise to a style of availability attack known as “unlearnable examples” (Feng et al., 2019; Shan et al., 2020; Huang et al., 2021; Fowl et al., 2021), wherein imperceptible changes are made to training data points, which nonetheless render them low value for use in ML model training. It has even led to the release of popular tools that serve this or a similar purpose (e.g., Glaze (Shan et al., 2023), Nightshade (Shan et al., 2024), and Mist (Liang et al., 2023)). These

*Equal contribution. †Aside from the first two authors, all other authors are listed in alphabetical order. ‡Correspondence to: Xiao-Shan Gao <xgao@mmrc.iss.ac.cn>.

offer public APIs (which we denote as \mathcal{P}) that allow a data owner to input their dataset \mathcal{D} and receive a “protected” version $\mathcal{D}' = \mathcal{P}(\mathcal{D})$.

We demonstrate that such black-box protection may give rise to an attack vector wherein an adversary can potentially render the protection ineffective. Specifically, given access to a small set \mathcal{D}_a of unprotected in-distribution data (e.g., data collected before protection is deployed; photos taken by others at a party; pictures of art taken at a gallery) and a public protection API \mathcal{P} , an adversary can easily acquire $(\mathcal{D}_a, \mathcal{P}(\mathcal{D}_a))$ pairs by querying the black-box service. We call such a risk *protection leakage*. In this paper, we aim to answer an intriguing question:

How can protection leakage sabotage data protection? And to what extent?

Indeed, with a small number of pairs, we show that an adversary can easily train a diffusion denoising bridge model (DDBM, Zhou et al., 2024) that learns an inverse mapping \mathcal{P}^{-1} such that $\mathcal{P}^{-1}(\mathcal{P}(\mathbf{x})) \approx \mathbf{x}$ for $\mathbf{x} \in \mathcal{D}_a$. Moreover, the learned bridge model generalizes to unseen data from the same distribution and can purify a large amount of protected data, i.e., \mathcal{D}' . We call this approach **BridgePure**. We show that, with the reasonable assumption of access to a small amount of protection leakage, our approach gives far better results than prior work (i.e., the original data is almost entirely recovered and maintains usability), and without requiring pre-training or fine-tuning a large diffusion model with a lot of data from a similar distribution. This demonstrates another critical vulnerability of data protection based on unlearnable examples.

In summary, our contributions are three-fold:

- We reveal the possible threat of protection leakage against black-box data protection methods;
- We propose *BridgePure* by utilizing DDBM as a powerful purification algorithm under the assumption of protection leakage;
- We conduct comprehensive experiments on purifying existing data protection methods for both classification tasks and generation tasks, where our method consistently outperforms baseline methods.

2 Background

In this section, we (1) introduce the goals and existing works of data protection on classification models and generative models; (2) outline existing countermeasures that may render the protections ineffective; (3) introduce diffusion bridge models, the key technique we will use throughout the paper.

2.1 Data Protection

Data protection in machine learning aims to achieve two goals: (1) Modify a raw dataset such that *it has low value to machine learning algorithms*; (2) Maintain *usability* for humans, such as publication purposes. We focus on data protection for images.

Formally, we denote the original dataset or *pre-protection* dataset as \mathcal{D} , and the *protected dataset* as \mathcal{D}' . We refer to the mapping from \mathcal{D} to \mathcal{D}' as *data protection* \mathcal{P} (e.g., an algorithm), where \mathcal{P} is applied to every entry in the dataset:

$$\mathcal{P} : \mathcal{D} \rightarrow \mathcal{D}', \mathbf{x} \mapsto \mathbf{x}'.$$

To preserve the visual semantics (thus preserve usability for humans), the mechanisms usually prevent modification from excessively degrading image quality, often relying on L_p -norm constraint: $\|\mathbf{x}' - \mathbf{x}\|_p \leq \varepsilon$.

Let \mathcal{M} be a training algorithm for a target task and $\mathcal{M}(\mathcal{D}')$ be a model trained using the protected dataset \mathcal{D}' . The protection mechanism \mathcal{P} is successful if $\mathcal{M}(\mathcal{D}')$ has degraded performance for the target task. In this paper, we consider two tasks: classification and style mimicry, and their corresponding protection.

Availability attacks. Availability attacks¹ can be regarded as a special case of data poisoning attacks. In the context of classification tasks, availability attacks subtly modify the original data, rendering the resulting model \mathcal{M} unusable by reducing its test accuracy to an unacceptable level. Thus, the protected data are often referred to as “unlearnable examples” (e.g., Huang et al., 2021).

Over the past few years, this field has advanced rapidly, demonstrating three key trends: (1) Improved performance: Recent techniques can reduce model availability to levels even lower than random guessing (Fowl et al., 2021; Chen et al., 2023). (2) Enhanced resilience: Availability attacks can be effective against both supervised and contrastive learning (He et al., 2023; Ren et al., 2023; Wang et al., 2024). Furthermore, robust unlearnable examples have been introduced to counteract weakened protections caused by adversarial training (Fu et al., 2022; Wen et al., 2023; Fang et al., 2024). (3) Transferable protection: Recent methods leverage image concepts and semantics to generate protective perturbations, enabling cross-dataset protection (Zhang et al., 2023; Chen et al., 2024). This remarkable progress highlights the potential of availability attacks as a practical data protection strategy in real-world applications.

Style mimicry protections. Consider an artist with artwork \mathcal{D} in a distinctive style \mathcal{S} . Modern latent diffusion models (LDMs) (Rombach et al., 2022) can readily fine-tune on \mathcal{D} to generate new images mimicking style \mathcal{S} from text prompts. To prevent such unauthorized style replication, data protection mechanisms \mathcal{P} modify the latent representation of \mathcal{D} to align with a different public dataset, making style extraction through LDM fine-tuning ineffective. In our analysis, we focus on two recent protection methods: Glaze (Shan et al., 2023) and Mist (Liang et al., 2023).

2.2 Circumventing Data Protection

To understand the real effectiveness of data protection, existing approaches propose techniques that degrade data protection. Specifically:

Purification-based methods. Adversarial purification was first introduced to sanitize adversarial examples at test time (Samangouei et al., 2018; Shi et al., 2021; Yoon et al., 2021). DiffPure (Nie et al., 2022) employs pre-trained diffusion models to remove undesired noise from the perturbed images. In the context of protection removal for classification tasks, AVATAR (Dolatabadi et al., 2024) borrows a diffusion model pre-trained on the unprotected dataset to purify the protected dataset. LE-JCDP (Jiang et al., 2023) fine-tunes a pre-trained diffusion model on additional data (i.e., the test set) and regularizes the sampling stage to improve the quality of purified images. D-VAE (Yu et al., 2024) leverages a variational auto-encoder-based method to disentangle protective perturbations from protected images, which requires no additional data. Regarding style mimicry tasks, Noisy Upscaling (Mustafa et al., 2019), DiffPure, and IMPRESS (Huang et al., 2024) prove effective in undermining the protection provided by current popular tools (Hönig et al., 2024).

Other methods². The imperceptible nature of protective modifications enables adversarial training to mitigate the protection efficacy for classification tasks (Madry et al., 2018; Tao et al., 2021). Additionally, processing the protected images by traditional and specially picked data augmentations can restore the availability to some extent (Liu et al., 2023; Qin et al., 2023; Zhu et al., 2024).

In this work, we show that under a realistic threat model of protection leakage, the strength of data protection can be almost completely diminished.

2.3 Diffusion Bridge Models

Denote by $q_{\text{data}}(\mathbf{x})$ the initial data distribution. We construct a diffusion process with a set of time-indexed variables $\{\mathbf{x}_t\}_{t=0}^T$. Diffusion models transporting the initial distribution to a standard Gaussian distribution

¹Note that while "availability attack" here refers to data protection methods, it can also mean indiscriminate data poisoning attacks. See Appendix A for a complete discussion.

²We discuss the line of work on showing current data protection shows a “false sense of security” in Appendix A.

are associated with the following SDE (Song et al., 2021):

$$d\mathbf{x}_t = \mathbf{f}(\mathbf{x}_t, t) dt + g(t) d\mathbf{w}_t, \quad \mathbf{x}_0 \sim q_{\text{data}}(\mathbf{x}) \quad (1)$$

where $\mathbf{f} : \mathbb{R}^d \times [0, T] \rightarrow \mathbb{R}^d$ is vector-valued drift function, $g : [0, T] \rightarrow \mathbb{R}$ is a scalar-valued diffusion coefficient and \mathbf{w}_t is a Wiener process.

We are interested in the transportation between two arbitrary data distributions. Assume the diffusion process $\{\mathbf{x}_t\}_{t=0}^T$ satisfies $\mathbf{x}_0 \sim q_{\text{data}}(\mathbf{x})$ and $\mathbf{x}_T = \mathbf{x}'$ as a fixed endpoint. This process can be modeled as the solution of the following SDE (Doob and Doob, 1984; Rogers and Williams, 2000):

$$d\mathbf{x}_t = \mathbf{f}(\mathbf{x}_t, t) dt + g^2(t) \mathbf{h}(\mathbf{x}_t, t, \mathbf{x}', T) + g(t) d\mathbf{w}_t, \quad \mathbf{x}_0 \sim q_{\text{data}}(\mathbf{x}), \mathbf{x}_T = \mathbf{x}' \quad (2)$$

where $\mathbf{h}(x, t, \mathbf{x}', T) = \nabla_{\mathbf{x}_t} \log p(\mathbf{x}_T | \mathbf{x}_t)|_{\mathbf{x}_t=x, \mathbf{x}_T=\mathbf{x}'}$ is the gradient of the log transition kernel of from t to T generated by the original SDE in eq. (1). One can reverse this process by deriving an SDE (Zhou et al., 2024):

$$d\mathbf{x}_t = [\mathbf{f}(\mathbf{x}_t, t) - g^2(t) (\frac{1}{2} \mathbf{s}(\mathbf{x}_t, t, \mathbf{x}', T) - \mathbf{h}(\mathbf{x}_t, t, \mathbf{x}', T))] dt + d\hat{\mathbf{w}}_t, \quad \mathbf{x}_T = \mathbf{x}', \quad (3)$$

where $\hat{\mathbf{w}}_t$ is a Wiener process and the score function $\mathbf{s}(x, t, \mathbf{x}', T) = \nabla_{\mathbf{x}_t} \log q(\mathbf{x}_t | \mathbf{x}_T)|_{\mathbf{x}_t=x, \mathbf{x}_T=\mathbf{x}'}$. The time-reversed SDE associated with a probability flow ODE :

$$d\mathbf{x}_t = [\mathbf{f}(\mathbf{x}_t, t) - g^2(t) (\frac{1}{2} \mathbf{s}(\mathbf{x}_t, t, \mathbf{x}', T) - \mathbf{h}(\mathbf{x}_t, t, \mathbf{x}', T))] dt, \quad (4)$$

Accordingly, a denoising diffusion bridge model (DDBM) parametrized by θ is trained by minimizing the following objective for score matching:

$$\mathcal{L}(\theta) = \mathbb{E}_{\mathbf{x}_t, \mathbf{x}_0, \mathbf{x}_T, t} [\omega(t) \|\mathbf{s}_\theta(\mathbf{x}_t, \mathbf{x}_T, t) - \nabla_{\mathbf{x}_t} \log q(\mathbf{x}_t | \mathbf{x}_0, \mathbf{x}_T)\|^2] \quad (5)$$

where $(\mathbf{x}_0, \mathbf{x}_T) \sim q_{\text{data}}(\mathbf{x}, \mathbf{x}')$, $\mathbf{x}_t \sim q(\mathbf{x}_t | \mathbf{x}_0, \mathbf{x}_T)$ and $\omega(t)$ is the weighting coefficient.

3 Threat Model

In this section, we introduce (1) how data protection provides service for individual data owners; (2) possible loopholes and an attack vector; (3) the notion of protection leakage, and (4) differences with existing works. Figure 1 summarizes the threat model considered in this paper.

Protection service. To leverage availability attacks for data protection, a black-box service can be offered to data owners without requiring machine learning expertise. For instance, Glaze (Shan et al., 2023) provides a user-friendly application where individuals can locally apply the protection mechanism \mathcal{P} to their personal dataset \mathcal{D} , generating a protected version \mathcal{D}' . In our work, we assume all attacks operate in a black-box manner, meaning both data owners and adversaries have no knowledge of \mathcal{P} 's internal mechanisms

Adversary. Note that while such black-box services are convenient for data owners, they are accessible to *anyone* without ownership verification. This means adversaries can potentially use these services to generate protected versions of data belonging to others. For instance, if there exist publicly available unprotected points belonging to a data owner, an adversary \mathcal{A} might use these unprotected points to form an additional dataset \mathcal{D}_a . Note that \mathcal{D}_a and \mathcal{D} must be drawn from similar distributions.

Formally, we define the adversary's capabilities as: (1) Access to a large dataset \mathcal{D}' of protected data; (2) Access to a small additional dataset \mathcal{D}_a of unprotected data, where $|\mathcal{D}_a| \ll |\mathcal{D}'|$ and $\mathcal{D}_a \cap \mathcal{D} = \emptyset$ (with \mathcal{D} being the original unprotected dataset corresponding to \mathcal{D}'); (3) Access to the black-box protection mechanism \mathcal{P} .

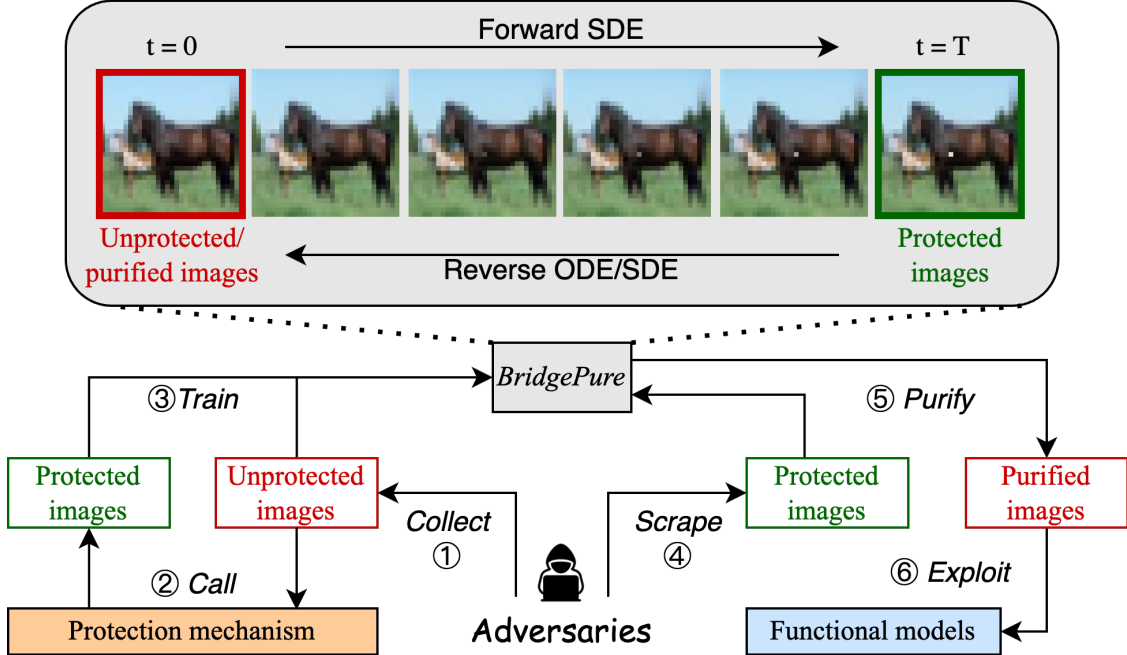


Figure 1: The threat model and illustration of BridgePure. Sequential images show the ODE sampling (purification) process of an example image protected by One-Pixel Shortcut (Wu et al., 2023).

Protection leakage. By querying the protection mechanism \mathcal{P} on the collected dataset \mathcal{D}_a , the adversary \mathcal{A} obtains a paired dataset:

$$\hat{\mathcal{D}}_a := \{(\mathbf{x}, \mathcal{P}(\mathbf{x})) | \mathbf{x} \in \mathcal{D}_a\}$$

containing both unprotected and protected versions of each data point. While \mathcal{P} remains black-box to \mathcal{A} , this paired dataset $\hat{\mathcal{D}}_a$ reveals information about the protection mechanism. For real-world applications of data protection, a critical question emerges: *Does the information leaked through $\hat{\mathcal{D}}_a$ compromise the protection provided by \mathcal{P} ?*

Our main finding reveals that protection leakage enables the construction of a powerful purification mechanism \mathcal{P}^{-1} that approximately reverses the protection \mathcal{P} . Using this mechanism, an adversary \mathcal{A} can purify the protected dataset \mathcal{D}' to obtain $\mathcal{P}^{-1}(\mathcal{D}')$, which closely matches the availability of the original dataset \mathcal{D} .

Difference with other purification methods. Notably, compared to existing circumvention methods discussed in Section 2.2, our approach is distinctive in two ways: (1) Our threat model assumes access to the black-box mechanism \mathcal{P} , providing the adversary greater (but viable) capabilities; (2) Our method requires only limited unprotected samples to develop a purification from scratch, unlike DiffPure (Nie et al., 2022) and AVATAR (Dolatabadi et al., 2024) for which models are pre-trained using enormous additional data.

4 Bridge Purification

In this section, we specify the possible impact of protection leakage by introducing Bridge Purification (*BridgePure*), a method that learns the inverse protection mechanism \mathcal{P}^{-1} from limited protection leakage $\hat{\mathcal{D}}_a = \{(\mathbf{x}, \mathbf{x}') | \mathbf{x} \in \mathcal{D}_a, \mathbf{x}' = \mathcal{P}(\mathbf{x})\}$, where each pair contains unprotected and protected versions of the same data. BridgePure works by modeling and then inverting the transformation between original and protected data.

Bridge training. Assume the pairs $(\mathbf{x}, \mathbf{x}')$ come from a joint distribution $q_{\text{data}}(\mathbf{x}, \mathbf{x}')$, where $\mathbf{x}' = \mathcal{P}(\mathbf{x})$. We aim to learn \mathcal{P}^{-1} that approximately samples from $q_{\text{data}}(\mathbf{x}|\mathbf{x}')$, i.e., purifying the protected data \mathbf{x}' . We first construct the stochastic process $\{\mathbf{x}_t\}_{t=0}^T$ that starts from $\mathbf{x}_0 = \mathbf{x}$ and ends at $\mathbf{x}_T = \mathbf{x}'$, where $q(\mathbf{x}_0, \mathbf{x}_T)$ approximates the true distribution $q_{\text{data}}(\mathbf{x}, \mathbf{x}')$. This process can be modeled by the SDE defined by eq. (2) in Section 2.3. We can reverse the process using the SDE and ODE defined by eq. (3) and eq. (4). Given the protection leakage $\widehat{\mathcal{D}}_a$, we train a denoising diffusion bridge model (Zhou et al., 2024) from scratch via minimizing the score-matching loss in eq. (5) on $\widehat{\mathcal{D}}_a$.

Sampling and purification. Different from standard diffusion models which perform unconditional sampling, BridgePure’s sampling process requires each step to be conditioned on the endpoint \mathbf{x}' (the protected data). Following Zhou et al. (2024), we deploy a hybrid sampling approach that combines Euler-Maruyama and Heun sampling methods, with a hyperparameter $s \in [0, 1]$ controlling the sampling randomness. When $s = 0$, the sampling is deterministic, and higher values of s introduce greater randomness. Note that choosing an appropriate s can enhance sampling quality and improve purified datasets’ availability, which we analyze through ablation studies on s in Section 5.4.

BridgePure purifies the protected dataset \mathcal{D}' by performing conditional sampling for each protected sample $\mathbf{x}' \in \mathcal{D}'$. As shown in Figure 1, the purification process gradually removes protective features, such as the white spot on the horse’s chest. After obtaining the purified dataset $\mathcal{P}^{-1}(\mathcal{D}')$, we evaluate purification effectiveness through model performance on the purified data, denoted as $\mathcal{M}(\mathcal{P}^{-1}(\mathcal{D}'))$.

Pre-processing. When $\widehat{\mathcal{D}}_a$ contains a small number of leaked pairs, BridgePure may overfit to the limited data and fail to generalize well to the protected dataset \mathcal{D}' . To address this limitation, we introduce Gaussian noise adding to the protected data, inspired by the diffusion process:

$$\mathcal{G}_\beta(\mathbf{x}') = \sqrt{1 - \beta}\mathbf{x}' + \sqrt{\beta}\mathbf{z}, \mathbf{z} \sim \mathcal{N}(0; 1).$$

After pre-processing, the protection leakage becomes $\widehat{\mathcal{D}}_a = \{(\mathbf{x}, \mathcal{G}_\beta(\mathbf{x}')) | \mathbf{x} \in \mathcal{D}_a, \mathbf{x}' = \mathcal{P}(\mathbf{x})\}$ and the protected dataset is $\mathcal{D}' = \{\mathcal{G}_\beta(\mathbf{x}') | \mathbf{x} \in \mathcal{D}, \mathbf{x}' = \mathcal{P}(\mathbf{x})\}$. BridgePure learns to model the transformation between \mathbf{x} and $\mathcal{G}_\beta(\mathbf{x}')$ using $\widehat{\mathcal{D}}_a$, then purifies $\mathcal{G}_\beta(\mathbf{x}') \in \mathcal{D}'$ by sampling approximately from $q_{\text{data}}(\mathbf{x}|\mathcal{G}_\beta(\mathbf{x}'))$. The effectiveness of BridgePure can be enhanced through the appropriate selection of the pre-processing parameter β , which we examine through ablation studies in Section 5.4.

5 Experiments

In this section, we (1) introduce our experimental setting; (2) present our purification results with BridgePure on purifying availability attacks and style mimicry protection; (3) ablation study of our approach.

5.1 Experimental Setting

Datasets. Our classification experiments use CIFAR-10/100 (Krizhevsky et al., 2012), ImageNet-Subset,³ WebFace-Subset,³ Cars (Krause et al., 2013), and Pets (Parkhi et al., 2012) datasets. For style mimicry experiments, we use artwork from artist *@nulevoy*,⁴ with details provided in Section 5.3.

Protections. On classification tasks, we leverage 14 availability attacks to simulate different data protection tools for classification tasks. Among them, AR (Sandoval-Segura et al., 2022) and LSP (Yu et al., 2022) are L_2 -norm attacks, OPS (Wu et al., 2023) is an L_0 -norm attack, while the rest are L_∞ -norm attacks including DC (Feng et al., 2019), EM (Huang et al., 2021), GUE (Liu et al., 2024), NTGA (Yuan and Wu, 2021),

³ImageNet-Subset is a subset of ImageNet (Deng et al., 2009) containing 100 classes. WebFace-Subset is a subset of CASIA-WebFace (Yi et al., 2014) containing 100 identities. See Appendix B.1 for detailed settings.

⁴<https://www.artstation.com/nulevoy>, usage with consent from the artist.

Table 1: Purification performance on CIFAR-10 and CIFAR-100 against nine availability attacks. The best restoration results are emphasized in **bold**. We underline to denote the least number of pairs required for BridgePure to surpass other baseline methods. We run five random trials for evaluation and report the mean value and standard deviation.

	AR	DC	EM	GUE	LSP	NTGA	OPS	REM	TAP
CIFAR-10 (94.01±0.15)									
Protected	13.52±0.63	15.10±0.81	23.79±0.13	12.76±0.44	13.85±0.96	12.87±0.23	13.67±1.80	20.96±1.70	9.51±0.67
PGD-AT	81.78±0.31	82.56±0.23	83.86±0.06	83.80±0.28	83.46±0.09	83.39±0.22	9.60±1.58	85.47±0.17	81.82±0.12
D-VAE	90.22±0.44	88.63±0.28	88.75±0.22	89.80±0.43	90.04±0.22	87.88±0.25	89.48±0.37	83.07±0.38	83.22±0.49
AVATAR	91.41±0.13	89.04±0.17	88.46±0.24	88.05±0.31	89.05±0.29	88.50±0.30	87.87±0.19	89.66±0.47	90.76±0.24
LE-JCDP	92.07±0.21	91.63±0.23	90.69±0.31	90.79±0.20	91.22±0.31	91.57±0.25	58.60±1.28	90.39±0.24	91.60±0.14
BridgePure-0.5K	93.86 ±0.27	93.76±0.17	<u>93.64</u> ±0.22	<u>93.70</u> ±0.11	<u>93.76</u> ±0.18	94.07 ±0.18	93.31±0.19	84.34±0.52	86.81±0.31
BridgePure-1K	92.48±0.11	93.78±0.25	93.73±0.15	93.80±0.20	93.84±0.19	93.94±0.08	93.49±0.26	<u>92.69</u> ±0.25	87.62±0.05
BridgePure-2K	93.84±0.22	93.93 ±0.20	93.81±0.22	93.97 ±0.15	93.99 ±0.34	94.00±0.16	93.31±0.36	93.49±0.18	88.60±0.22
BridgePure-4K	93.56±0.21	93.81±0.05	93.87 ±0.15	93.84±0.21	93.93±0.27	93.93±0.12	93.50 ±0.28	93.50 ±0.11	92.91 ±0.12
CIFAR-100 (74.27±0.45)									
Protected	2.02±0.12	36.10±0.67	6.73±0.12	19.50±0.48	2.56±0.16	1.51±0.22	12.18±0.52	7.07±0.19	3.59±0.12
PGD-AT	56.37±0.25	55.21±0.40	56.25±0.29	57.38±0.27	56.19±0.28	54.77±0.25	7.59±0.32	56.81±0.19	54.59±0.28
D-VAE	62.14±0.32	55.91±0.92	60.25±0.25	60.79±0.62	61.36±0.75	59.34±0.64	62.83±0.67	63.06±0.31	53.82±0.91
AVATAR	65.45±0.32	63.48±0.26	62.77±0.56	62.10±0.22	62.95±0.38	62.60±0.22	60.68±0.56	65.36±0.38	64.50±0.23
LE-JCDP	69.15±0.22	68.49±0.42	67.76±0.31	67.36±0.42	68.23±0.40	68.35±0.19	39.10±0.40	68.76±0.23	68.39±0.39
BridgePure-0.5K	67.49±0.31	<u>73.69</u> ±0.21	<u>73.17</u> ±0.13	<u>72.69</u> ±0.49	<u>73.33</u> ±0.77	<u>69.11</u> ±0.86	74.18 ±0.31	66.53±0.29	62.75±0.25
BridgePure-1K	68.63±0.84	73.62±0.34	73.31±0.42	72.92±0.62	73.93±0.24	69.96±0.47	74.22±0.30	66.30±0.36	62.58±0.28
BridgePure-2K	68.05±0.16	73.83±0.15	73.70 ±0.30	73.55±0.29	73.86±0.56	73.90±0.19	73.96±0.40	<u>72.38</u> ±0.44	64.96±0.27
BridgePure-4K	72.44 ±0.47	73.97 ±0.18	73.52±0.57	73.92 ±0.09	74.56 ±0.40	74.23 ±0.23	74.18 ±0.38	72.95 ±0.10	70.96 ±0.15

Table 2: Purification performance on ImageNet-Subset and WebFace-Subset against three availability attacks.

	EM	LSP	TAP	EM	LSP	TAP
ImageNet-Subset (66.18±0.60)			WebFace-Subset (87.84±0.27)			
Protected	6.83±0.68	26.77±1.49	17.48±0.81	1.72±0.06	2.33±0.44	3.24±0.52
DiffPure	54.87±0.36	56.31±0.47	62.03±0.34	86.54±0.16	78.01±0.21	79.59±0.79
BridgePure-0.5K	<u>65.89</u> ±0.53	<u>65.74</u> ±0.31	<u>62.76</u> ±0.31	87.80 ±0.42	87.80 ±0.27	82.48±0.23
BridgePure-1K	65.66±0.38	66.02±0.50	63.89±0.38	87.76±0.20	87.67±0.37	86.38±0.26
BridgePure-2K	65.96±0.49	65.88±0.35	63.96±0.47	87.77±0.40	87.72±0.24	87.27±0.42
BridgePure-4K	66.02 ±0.55	66.27 ±0.52	64.34 ±0.51	87.60±0.12	87.64±0.26	87.46 ±0.19

REM (Fu et al., 2022), TAP (Fowl et al., 2021), CP (He et al., 2023), TUE (Ren et al., 2023), AUE (Wang et al., 2024), UC and UC-CLIP (Zhang et al., 2023). If not otherwise stated, these L_∞ -norm attacks use a modification budget $\varepsilon = 8/255$. More details about protection generation are available in Appendix B.2. On generation tasks, we deploy two style mimicry protection tools, i.e., Glaze v2.1 (Shan et al., 2023) and Mist (Liang et al., 2023).

BridgePure. We train BridgePure using a small set of (unprotected, protected) pairs to purify large-scale protected data and evaluate the purified dataset’s availability. We denote BridgePure- N as the model trained on N pairs, ensuring these training pairs are distinct from the protected samples to be purified. Following Section 4, we apply Gaussian perturbation with parameter β during pre-processing and control sampling randomness via parameter s . For CIFAR-10 and CIFAR-100, we report BridgePure’s best performance across four configurations: $s \in \{0.33, 0.8\}$ and $\beta \in \{0, 0.02\}$. For ImageNet-Subset, WebFace-Subset, Cars, and Pets, we report results with $s \in \{0.33, 0.8\}$ and $\beta = 0$. For style mimicry protection, we set $s = \beta = 0$.

Purification baselines. We compare BridgePure with existing purification-based methods in Section 2.2, including adversarial training (Madry et al., 2018) and three purification baselines including D-VAE (Yu et al., 2024), AVATAR (Dolatabadi et al., 2024), and LE-JCDP (Jiang et al., 2023) on CIFAR-10 and CIFAR-100. Notably, D-VAE requires no additional data, while AVATAR uses a diffusion model trained on the unprotected training set (50K images), and LE-JCDP fine-tunes a diffusion model on the unprotected test set (10K images). For ImageNet-Subset and WebFace-Subset comparisons with DiffPure (Nie et al., 2022), details are provided in the relevant section.

5.2 Purifying Availability Attacks

Main results. We evaluate four levels of protection leakage: $N = 500, 1000, 2000,$ and 4000 pairs of unprotected and protected images. For each level, an adversary trains a BridgePure model to attempt purification of the protected dataset. In Table 1, we compare BridgePure with four baseline methods: adversarial training using PGD-10 with budget $8/255$ in L_∞ -norm, D-VAE, AVATAR, and LE-JCDP. The results demonstrate the significant impact of protection leakage in three aspects: (1) *Restoration with limited leakage:* BridgePure substantially restores dataset availability even with a few leaked pairs. (2) *Superior performance with higher budgets:* Using up to 4K pairs, BridgePure consistently outperforms all baseline methods across nine attacks. (3) *Closing the availability gap:* BridgePure’s protection-specific design increasingly eliminates the availability gap, approaching perfect restoration as protection leakage increases.

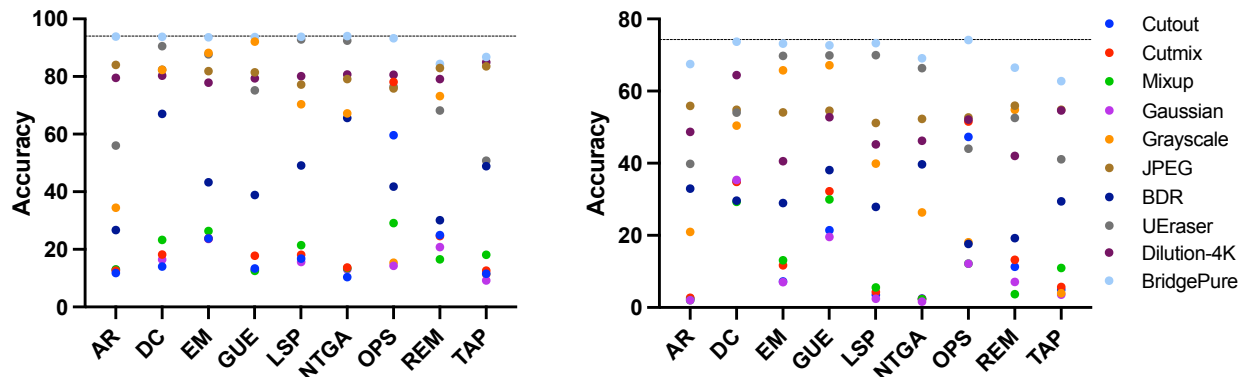


Figure 2: Comparison between BridgePure-0.5K and augmentation-based methods as well as protection dilution on CIFAR-10 (left) and CIFAR-100 (right). The dashed lines represent the unprotected baselines.

Moreover, Figure 2 demonstrates that BridgePure-0.5K consistently outperforms augmentation-based circumvention methods. We also considered the scenario where the adversary dilutes the protected dataset with a sufficiently large amount of unprotected data. The results indicate that 500 leaked pairs have a significantly greater destructive impact and harm than 4,000 leaked unprotected samples.

Table 3: Purification performance on Cars and Pets against two label-agnostic availability attacks.

	UC	UC-CLIP	UC	UC-CLIP
	Cars (43.25±1.71)		Pets (49.56±0.81)	
Protected	25.91±4.58	10.93±2.78	20.91±1.17	24.07±4.92
BridgePure-0.5K	43.65±1.32	42.72±1.64	50.03±0.80	50.70±1.44
BridgePure-1K	42.32±1.25	43.45±2.44	49.27±3.08	49.75±0.78

In Table 2, we evaluate BridgePure on ImageNet-Subset and WebFace-Subset to illustrate the risk of

protection leakage in real-world scenarios. For baseline DiffPure, the diffusion model for ImageNet-Subset is trained on the entire ImageNet and that for WebFace-Subset is trained on CelebA (Liu et al., 2015). We report the best results of DiffPure among four selections of sampling step, i.e., $t^* \in \{0.1, 0.2, 0.3, 0.4\}$. When the amount of leaked pairs is 500, our BridgePure already surpasses DiffPure on the two datasets. Moreover, BridgePure can restore the availability to the original levels as the leakage grows.

Label-agnostic case. We consider label-agnostic variants of availability attacks, i.e., UC and UC-CLIP, whose protection generation depends on clustering in the feature space of a pre-trained encoder such as CLIP (Radford et al., 2021). We adopt their default implementation settings where the number of surrogate clusters is 10 and the protection budget is $16/255$ in L_∞ norm. In Table 3, BridgePure with at most 1000 leaked pairs can purify the protected datasets to the original availability levels.

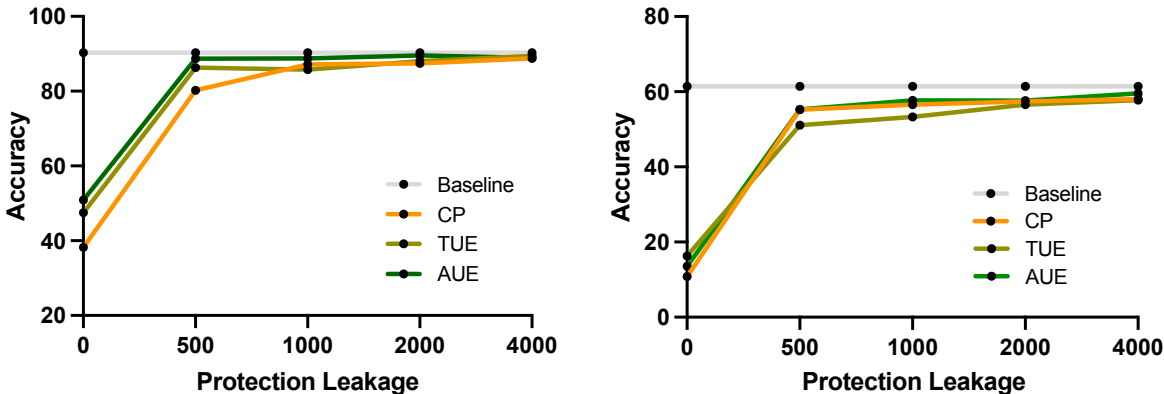


Figure 3: Purification performance on CIFAR-10 (left) and CIFAR-100 (right) against three availability attacks that SimCLR evaluates.

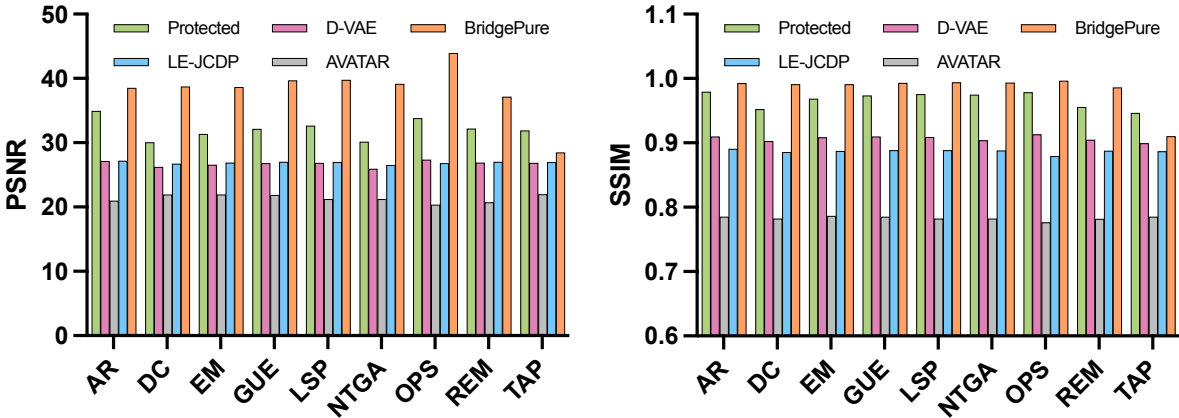


Figure 4: Peak Signal-to-Noise Ratio (PSNR, left) and Structural Similarity Index Measure (SSIM, right) between processed datasets and original CIFAR-10. The larger these two metrics, the more similar the processed dataset is to the original one. Here our method is BridgePure-1K.

Contrastive learning case. We consider availability attacks that transfer to contrastive learning algorithms. We purify CP, TUE, and AUE by BridgePure and then train classifiers using SimCLR (Chen et al., 2020) and



Figure 5: Purification outcomes on UC-protected Cars dataset. The **top** row is the overview comparison and the **bottom** row shows local details around the wheel. We point out (1) the light, (2) the tire, and (3) the wheel hub where BridgePure-0.5K preserves the original texture while DiffPure ($t^* = 0.2$) blurs the details.

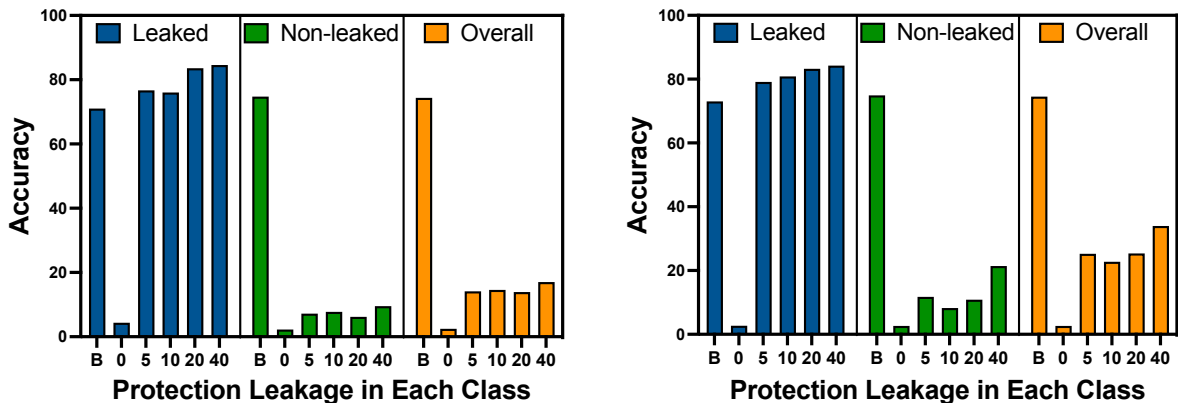


Figure 6: Performance with partial protection leakage within 10 classes (**left**) and 20 classes (**right**) of LSP-protected CIFAR-100. The **x-axis** represents the number of leaked pairs in each leaked class and “B” stands for the unprotected baseline. Here $s = 0.33$ and $\beta = 0$.

linear probing. Figure 3 shows that limited protection leakage enables BridgePure to recover the availability for contrastive learning significantly.

Purified image quality. A distinct feature of BridgePure is its conditional generation based on the protected images. We observe that this approach enables high-quality restoration, preserves image details, and avoids artificial distortions or artifacts.

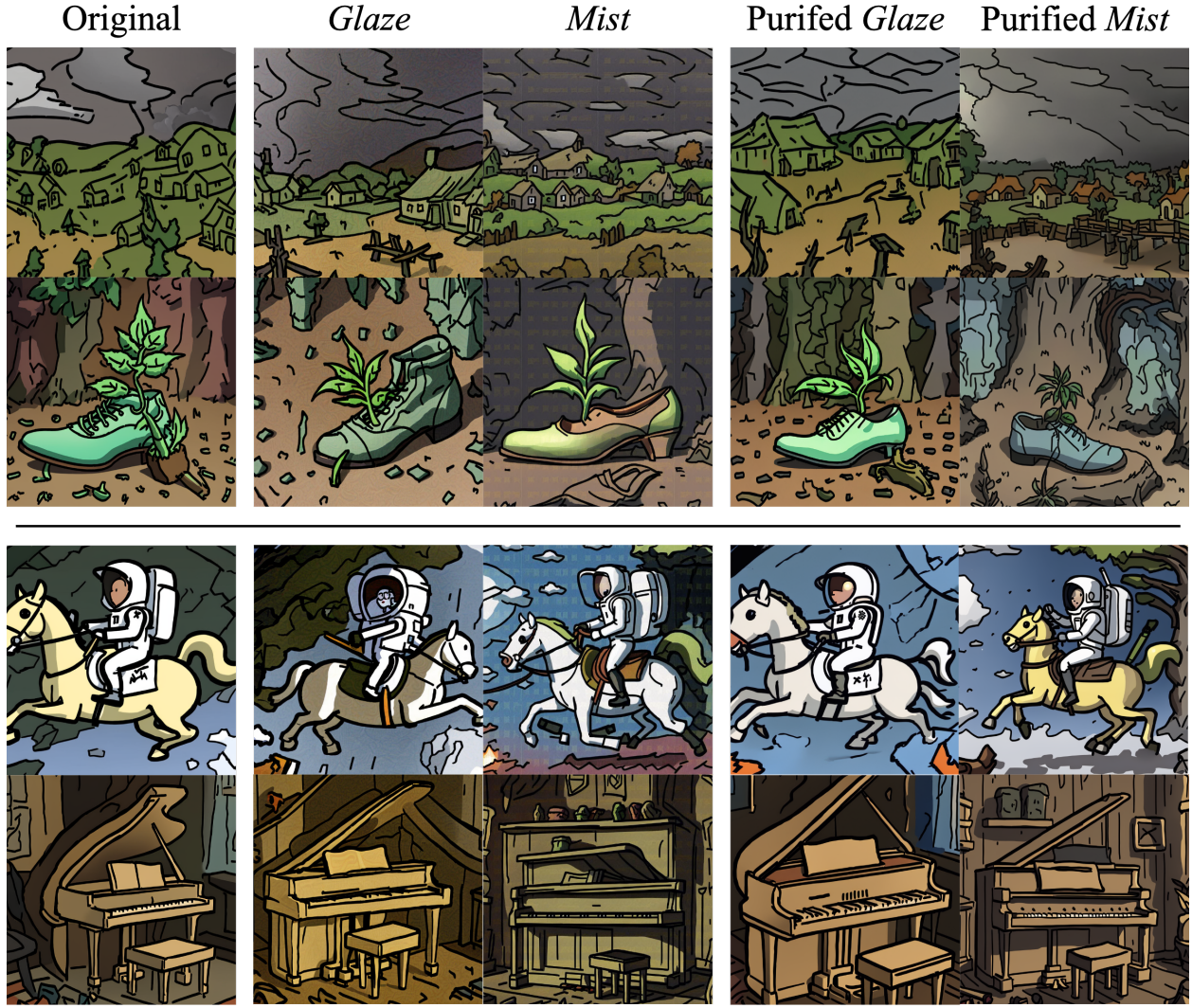


Figure 7: Purification performance of BridgePure-5 (**top**) and BridgePure-10 (**bottom**) for style mimicry. The presented paintings are mimicry outcomes of fine-tuned generative models.

Specifically, in Figure 4, we evaluate the similarity between the original (unprotected) data and their purified versions with PSNR and SSIM metrics. We also present the similarity between the protected and unprotected pairs as a baseline before purification. We observe that our method outperforms all baseline purification methods in terms of restoring the unprotected data. Moreover, our method consistently improves image similarity through purification, while other methods would downgrade the similarity compared with the protected baseline.

Moreover, in Figure 5, we compare the details of the purified images generated by DiffPure and BridgePure. In terms of the purification mechanism, DiffPure adds Gaussian noise to protected images and aligns them with learned trajectories before reverse sampling. We observe such an unconditional process could cause the loss of texture details. In contrast, BridgePure’s conditional sampling preserves fine-grained features. Concretely, details of the vehicle purified by BridgePure, such as lights, tires, and wheel hubs are in sharper clarity than those purified by DiffPure.

Partial protection leakage. We consider a scenario where the adversary aims to purify protected images from certain classes rather than the whole protected dataset \mathcal{D}' . In Figure 6, we purify LSP-protected CIFAR-100 using partial protection leakage within 10/20 random classes and report the accuracy of leaked, non-leaked, and all classes, respectively. The results demonstrate that partial protection leakage poses an even more significant risk to relevant classes. For example, 5 pairs from each class are sufficient to make the test accuracy of the target classes better than the unprotected baseline and more pairs will improve it further.

Mixture of protection. The mechanism \mathcal{P} could possibly employ multiple availability attacks to protect data. In such cases, the protection leakage also contains a mixture of differently protected pairs. In Table 4, we consider a scenario in which \mathcal{P} randomly applies one of five attacks to a given input data. We observe that, firstly, the mixture of protection harms the protection performance and this approach is not desirable; secondly, BridgePure is still very effective in restoring availability when the leakage amount is relatively small.

Table 4: Purification performance in the mixed-attacks scenario, where five availability attacks including AR, EM, LSP, OPS, and TAP are randomly applied for data protection.

	Protected	BridgePure		
		0.25K	0.5K	1K
CIFAR-10 (94.01±0.15)	61.60±1.78	93.00±0.26	93.14±0.24	93.01±0.20
CIFAR-100 (74.27±0.45)	51.57±2.15	71.31±0.50	72.00±0.24	72.77±0.33

5.3 Purifying Style Mimicry Protection

In this section, we investigate the threat of protection leakage to copyright protection for generative models. We consider art style mimicry on the artwork from an artist *@nulevoy* with consent. We first fine-tune Stable Diffusion v2.1 (Rombach et al., 2022) using 20 captioned paintings following the implementation of Hönig et al. (2024). We then reproduce the style of the artist with a list of prompts during inference. Our implementation details are available in Appendix B.5.

For style mimicry protection, we apply Glaze and Mist to protect the 20 paintings we used previously. We assume protection leakage of only 5 or 10 unprotected paintings of the same artist and call these public protection tools to obtain (unprotected, protected) pairs for BridgePure training. Finally, the 20 protected paintings are purified by BridgePure and fed into the style mimicry pipeline.

Figures 7 and 10 show the style mimicry outcomes given different text prompts. Models fine-tuned on Glaze-protected artwork produce images filled with irregular patterns, while artwork protected by Mist leads fine-tuned models to generate artistic works with regular block-like perturbations. After purification by BridgePure, images protected by Glaze and Mist can no longer cause fine-tuned models to generate artwork with protective cloaks. Our results again suggest that for style mimicry, protection leakage poses a strong threat to existing data protection tools.

5.4 Ablation Study

Figure 8 shows that pre-processing with Gaussian noise can improve the availability restoration against some availability attacks which are “harder” to purify, e.g., TAP. However, it also presents a performance ceiling for other protections, e.g., EM and LSP, and harms their purification results. Regarding the sampling randomness, while larger randomness slightly reduces the accuracy for some protections, e.g., EM, LSP, and OPS, it can largely benefit the purification against TAP, REM, and AR.

In summary, different protection methods are subject to different choices of the optimal hyperparameter. Our results in this section reveal the worst-case damage caused by protection leakage by reporting the best-performing BridgePure within a limited number of trials.

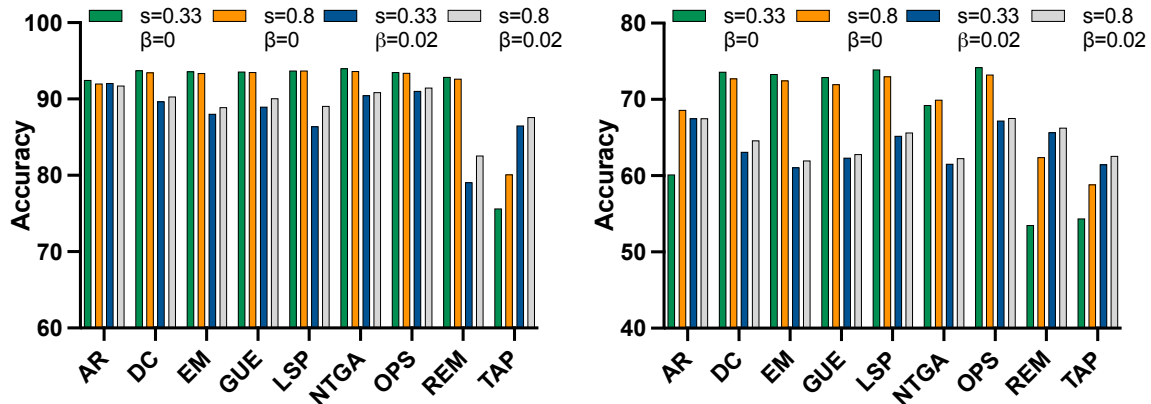


Figure 8: Influence of s and β on BridgePure-1K performance on CIFAR-10 (left) and CIFAR-100 (right).

6 Conclusion

In this paper, we identify a critical vulnerability in black-box data protection systems: *protection leakage*. We demonstrate that using a small number of leaked pairs, an adversary can train a diffusion bridge model, *BridgePure*, to effectively circumvent the protection mechanism. Our empirical results show that under this threat model, *BridgePure* exposes fundamental vulnerabilities in current data protection systems for both classification and generation tasks.

Limitations and future work. Our findings highlight the necessity of addressing protection leakage. At the system level, protection services should incorporate robust identity authentication mechanisms to verify data ownership. At the algorithmic level, enhanced protection methods must be developed to strengthen resistance against advanced purification techniques.

Acknowledgment

We sincerely thank Stanislav Voloshin (@nulevoy) for his permission to present experimental results based on his artwork in our paper. GK and YY gratefully acknowledge NSERC and CIFAR for funding support.

References

- Aghakhani, H., D. Meng, Y.-X. Wang, C. Kruegel, and G. Vigna (2021). “Bullseye polytope: A scalable clean-label poisoning attack with improved transferability”. In: *IEEE European Symposium on Security and Privacy (EuroS&P)*, pp. 159–178.
- Biggio, B., B. Nelson, and P. Laskov (2012). “Poisoning attacks against support vector machines”. In: *Proceedings of the 29th International Conference on Machine Learning (ICML)*, pp. 1467–1474.
- Chen, C., J. Zhang, Y. Li, and Z. Han (2024). “One for All: A Universal Generator for Concept Unlearnability via Multi-Modal Alignment”. In: *Forty-first International Conference on Machine Learning*.
- Chen, S., G. Yuan, X. Cheng, Y. Gong, M. Qin, Y. Wang, and X. Huang (2023). “Self-Ensemble Protection: Training Checkpoints Are Good Data Protectors”. In: *The Eleventh International Conference on Learning Representations*.
- Chen, T., S. Kornblith, M. Norouzi, and G. Hinton (2020). “A simple framework for contrastive learning of visual representations”. In: *International conference on machine learning*. PMLR, pp. 1597–1607.
- Chen, X., C. Liu, B. Li, K. Lu, and D. Song (2017). “Targeted backdoor attacks on deep learning systems using data poisoning”. arXiv:1712.05526.
- Deng, J., W. Dong, R. Socher, L.-J. Li, K. Li, and L. Fei-Fei (2009). “Imagenet: A large-scale hierarchical image database”. In: *2009 IEEE conference on computer vision and pattern recognition*. Ieee, pp. 248–255.
- Dolatabadi, H. M., S. Erfani, and C. Leckie (2024). “The devil’s advocate: Shattering the illusion of unexploitable data using diffusion models”. In: *2024 IEEE Conference on Secure and Trustworthy Machine Learning (SaTML)*. IEEE, pp. 358–386.
- Doob, J. L. and J. Doob (1984). “Classical potential theory and its probabilistic counterpart”. Vol. 262. Springer.
- Dosovitskiy, A. et al. (2021). “An Image is Worth 16x16 Words: Transformers for Image Recognition at Scale”. In: *International Conference on Learning Representations*.
- Fang, B., B. Li, S. Wu, S. Ding, T. Zheng, R. Yi, and L. Ma (2024). “Collapsing the Learning: Crafting Broadly Transferable Unlearnable Examples”.
- Feng, J., Q.-Z. Cai, and Z.-H. Zhou (2019). “Learning to confuse: Generating training time adversarial data with auto-encoder”. *Advances in Neural Information Processing Systems*, vol. 32.
- Fowl, L., M. Goldblum, P.-y. Chiang, J. Geiping, W. Czaja, and T. Goldstein (2021). “Adversarial examples make strong poisons”. In: *Advances in Neural Information Processing Systems*. Vol. 34, pp. 30339–30351.
- Fu, S., F. He, Y. Liu, L. Shen, and D. Tao (2022). “Robust Unlearnable Examples: Protecting Data Privacy Against Adversarial Learning”. In: *International Conference on Learning Representations*.
- Geiping, J., L. H. Fowl, W. R. Huang, W. Czaja, G. Taylor, M. Moeller, and T. Goldstein (2021). “Witches’ Brew: ial Scale Data Poisoning via Gradient Matching”. In: *International Conference on Learning Representations*.
- Gu, T., B. Dolan-Gavitt, and S. Garg (2017). “Badnets: Identifying vulnerabilities in the machine learning model supply chain”. arXiv:1708.06733.

- Guo, J. and C. Liu (2020). “Practical Poisoning Attacks on Neural Networks”. In: *European Conference on Computer Vision*, pp. 142–158.
- He, H., K. Zha, and D. Katabi (2023). “Indiscriminate Poisoning Attacks on Unsupervised Contrastive Learning”. In: *The Eleventh International Conference on Learning Representations*.
- Hill, K. (2023). “Your Face Belongs to Us: The Secretive Startup Dismantling Your Privacy”. Simon and Schuster.
- Hönig, R., J. Rando, N. Carlini, and F. Tramèr (2024). “Adversarial Perturbations Cannot Reliably Protect Artists From Generative AI”. *arXiv preprint arXiv:2406.12027*.
- Hu, J., L. Shen, and G. Sun (2018). “Squeeze-and-excitation networks”. In: *Proceedings of the IEEE conference on computer vision and pattern recognition*, pp. 7132–7141.
- Huang, G., Z. Liu, L. Van Der Maaten, and K. Q. Weinberger (2017). “Densely connected convolutional networks”. In: *Proceedings of the IEEE conference on computer vision and pattern recognition*, pp. 4700–4708.
- Huang, H., X. Ma, S. M. Erfani, J. Bailey, and Y. Wang (2021). “Unlearnable Examples: Making Personal Data Unexploitable”. In: *ICLR*.
- Huang, J., Z. Guo, G. Luo, Z. Qian, S. Li, and X. Zhang (2024). “Disentangled Style Domain for Implicit $\$z\$$ -Watermark Towards Copyright Protection”. In: *The Thirty-eighth Annual Conference on Neural Information Processing Systems*.
- Jiang, W., Y. Diao, H. Wang, J. Sun, M. Wang, and R. Hong (2023). “Unlearnable examples give a false sense of security: Piercing through unexploitable data with learnable examples”. In: *Proceedings of the 31st ACM International Conference on Multimedia*, pp. 8910–8921.
- Koh, P. W. and P. Liang (2017). “Understanding black-box predictions via influence functions”. In: *Proceedings of the 34th International Conference on Machine Learning (ICML)*, pp. 1885–1894.
- Koh, P. W., J. Steinhardt, and P. Liang (2022). “Stronger Data Poisoning Attacks Break Data Sanitization Defenses”. *Machine Learning*, vol. 111, pp. 1–47.
- Krause, J., M. Stark, J. Deng, and L. Fei-Fei (2013). “3D Object Representations for Fine-Grained Categorization”. In: *4th International IEEE Workshop on 3D Representation and Recognition (3dRR-13)*. Sydney, Australia.
- Krizhevsky, A., I. Sutskever, and G. E. Hinton (2012). “Imagenet classification with deep convolutional neural networks”. *Advances in neural information processing systems*, vol. 25.
- Li, J., D. Li, S. Savarese, and S. Hoi (2023). “Blip-2: Bootstrapping language-image pre-training with frozen image encoders and large language models”. In: *International conference on machine learning*. PMLR, pp. 19730–19742.
- Liang, C., X. Wu, Y. Hua, J. Zhang, Y. Xue, T. Song, Z. Xue, R. Ma, and H. Guan (2023). “Adversarial example does good: Preventing painting imitation from diffusion models via adversarial examples”. In: *International Conference on Machine Learning*. PMLR, pp. 20763–20786.
- Liu, S., Y. Wang, and X.-S. Gao (2024). “Game-theoretic unlearnable example generator”. In: *Proceedings of the AAAI Conference on Artificial Intelligence*. Vol. 38. 19, pp. 21349–21358.

- Liu, Z., Z. Zhao, and M. Larson (2023). “Image shortcut squeezing: Countering perturbative availability poisons with compression”. In: *International conference on machine learning*. PMLR, pp. 22473–22487.
- Liu, Z., P. Luo, X. Wang, and X. Tang (2015). “Deep Learning Face Attributes in the Wild”. In: *Proceedings of International Conference on Computer Vision (ICCV)*.
- Lu, Y., G. Kamath, and Y. Yu (2022). “Indiscriminate Data Poisoning Attacks on Neural Networks”. *Transactions on Machine Learning Research*.
- (2023). “Exploring the Limits of Model-Targeted Indiscriminate Data Poisoning Attacks”. In: *Proceedings of the 40th International Conference on Machine Learning*.
- Lu, Y., M. Y. Yang, G. Kamath, and Y. Yu (2024). “Indiscriminate Data Poisoning Attacks on Pre-trained Feature Extractors”. In: *2024 IEEE Conference on Secure and Trustworthy Machine Learning (SaTML)*. IEEE, pp. 327–343.
- Madry, A., A. Makelov, L. Schmidt, D. Tsipras, and A. Vladu (2018). “Towards Deep Learning Models Resistant to Adversarial Attacks”. In: *International Conference on Learning Representations*.
- Muñoz-González, L., B. Biggio, A. Demontis, A. Paudice, V. Wongrassamee, E. C. Lupu, and F. Roli (2017). “Towards Poisoning of Deep Learning Algorithms with Back-gradient Optimization”. In: *Proceedings of the 10th ACM Workshop on Artificial Intelligence and Security (AISec)*.
- Mustafa, A., S. H. Khan, M. Hayat, J. Shen, and L. Shao (2019). “Image super-resolution as a defense against adversarial attacks”. *IEEE Transactions on Image Processing*, vol. 29, pp. 1711–1724.
- Nie, W., B. Guo, Y. Huang, C. Xiao, A. Vahdat, and A. Anandkumar (2022). “Diffusion models for adversarial purification”. In: *International Conference on Machine Learning (ICML)*.
- Parkhi, O. M., A. Vedaldi, A. Zisserman, and C. V. Jawahar (2012). “Cats and Dogs”. In: *IEEE Conference on Computer Vision and Pattern Recognition*.
- Pooladzandi, O., S. G. Bhat, J. Jiang, A. Branch, and G. Pottie (2024). “PureGen: Universal Data Purification for Train-Time Poison Defense via Generative Model Dynamics”. In: *The Thirty-eighth Annual Conference on Neural Information Processing Systems*.
- Qin, T., X. Gao, J. Zhao, K. Ye, and C.-Z. Xu (2023). “Learning the unlearnable: Adversarial augmentations suppress unlearnable example attacks”. In: *4th Workshop on Adversarial Robustness In the Real World (AROW), ICCV 2023*.
- Radford, A. et al. (2021). “Learning transferable visual models from natural language supervision”. In: *International conference on machine learning*. PMLR, pp. 8748–8763.
- Radiya-Dixit, E., S. Hong, N. Carlini, and F. Tramèr (2022). “Data Poisoning Won’t Save You From Facial Recognition”. In: *International Conference on Learning Representations*.
- Ren, J., H. Xu, Y. Wan, X. Ma, L. Sun, and J. Tang (2023). “Transferable Unlearnable Examples”. In: *The Eleventh International Conference on Learning Representations*.
- Rogers, L. C. G. and D. Williams (2000). “Diffusions, Markov processes, and martingales: Itô calculus”. Vol. 2. Cambridge university press.
- Rombach, R., A. Blattmann, D. Lorenz, P. Esser, and B. Ommer (2022). “High-Resolution Image Synthesis With Latent Diffusion Models”. In: *Proceedings of the IEEE/CVF Conference on Computer Vision and Pattern Recognition (CVPR)*, pp. 10684–10695.

- Saha, A., A. Subramanya, and H. Pirsiavash (2020). “Hidden trigger backdoor attacks”. In: *Proceedings of the AAAI Conference on Artificial Intelligence*.
- Samangouei, P., M. Kabkab, and R. Chellappa (2018). “Defense-GAN: Protecting Classifiers Against Adversarial Attacks Using Generative Models”. In: *International Conference on Learning Representations*.
- Sandler, M., A. Howard, M. Zhu, A. Zhmoginov, and L.-C. Chen (2018). “Mobilenetv2: Inverted residuals and linear bottlenecks”. In: *Proceedings of the IEEE conference on computer vision and pattern recognition*, pp. 4510–4520.
- Sandoval-Segura, P., V. Singla, J. Geiping, M. Goldblum, T. Goldstein, and D. Jacobs (2022). “Autoregressive Perturbations for Data Poisoning”. In: *Advances in Neural Information Processing Systems*. Ed. by S. Koyejo, S. Mohamed, A. Agarwal, D. Belgrave, K. Cho, and A. Oh. Vol. 35. Curran Associates, Inc., pp. 27374–27386.
- Shafahi, A., W. R. Huang, M. Najibi, O. Suci, C. Studer, T. Dumitras, and T. Goldstein (2018). “Poison Frogs! Targeted Clean-Label Poisoning Attacks on Neural Networks”. In: *Advances in Neural Information Processing Systems (NeurIPS)*, pp. 6103–6113.
- Shan, S., J. Cryan, E. Wenger, H. Zheng, R. Hanocka, and B. Y. Zhao (2023). “Glaze: Protecting artists from style mimicry by {Text-to-Image} models”. In: *32nd USENIX Security Symposium (USENIX Security 23)*, pp. 2187–2204.
- Shan, S., W. Ding, J. Passananti, S. Wu, H. Zheng, and B. Y. Zhao (2024). “Nightshade: Prompt-Specific Poisoning Attacks on Text-to-Image Generative Models”. In: *2024 IEEE Symposium on Security and Privacy (SP)*. IEEE Computer Society, pp. 212–212.
- Shan, S., E. Wenger, J. Zhang, H. Li, H. Zheng, and B. Y. Zhao (2020). “Fawkes: Protecting privacy against unauthorized deep learning models”. In: *29th USENIX security symposium (USENIX Security 20)*, pp. 1589–1604.
- Shi, C., C. Holtz, and G. Mishne (2021). “Online Adversarial Purification based on Self-supervised Learning”. In: *International Conference on Learning Representations*.
- Song, Y., J. Sohl-Dickstein, D. P. Kingma, A. Kumar, S. Ermon, and B. Poole (2021). “Score-Based Generative Modeling through Stochastic Differential Equations”. In: *International Conference on Learning Representations*.
- Suya, F., S. Mahloujifar, A. Suri, D. Evans, and Y. Tian (2021). “Model-targeted poisoning attacks with provable convergence”. In: *Proceedings of the 38th International Conference on Machine Learning*, pp. 10000–10010.
- Tao, L., L. Feng, J. Yi, S.-J. Huang, and S. Chen (2021). “Better safe than sorry: Preventing delusive adversaries with adversarial training”. *Advances in Neural Information Processing Systems*, vol. 34, pp. 16209–16225.
- Touvron, H., M. Cord, A. Sablayrolles, G. Synnaeve, and H. Jégou (2021). “Going deeper with image transformers”. In: *Proceedings of the IEEE/CVF international conference on computer vision*, pp. 32–42.
- Tran, B., J. Li, and A. Madry (2018). “Spectral Signatures in Backdoor Attacks”. In: *Advances in Neural Information Processing Systems (NeurIPS)*.

- Wang, Y., Y. Zhu, and X.-S. Gao (2024). “Efficient Availability Attacks against Supervised and Contrastive Learning Simultaneously”. In: *The Thirty-eighth Annual Conference on Neural Information Processing Systems*.
- Wen, R., Z. Zhao, Z. Liu, M. Backes, T. Wang, and Y. Zhang (2023). “Is Adversarial Training Really a Silver Bullet for Mitigating Data Poisoning?” In: *The Eleventh International Conference on Learning Representations*.
- Wu, S., S. Chen, C. Xie, and X. Huang (2023). “One-Pixel Shortcut: On the Learning Preference of Deep Neural Networks”. In: *The Eleventh International Conference on Learning Representations*.
- Yi, D., Z. Lei, S. Liao, and S. Z. Li (2014). “Learning face representation from scratch”. *arXiv preprint arXiv:1411.7923*.
- Yoon, J., S. J. Hwang, and J. Lee (2021). “Adversarial purification with score-based generative models”. In: *International Conference on Machine Learning*. PMLR, pp. 12062–12072.
- Yu, D., H. Zhang, W. Chen, J. Yin, and T.-Y. Liu (2022). “Availability attacks create shortcuts”. In: *Proceedings of the 28th ACM SIGKDD Conference on Knowledge Discovery and Data Mining*, pp. 2367–2376.
- Yu, Y., Y. Wang, S. Xia, W. Yang, S. Lu, Y.-p. Tan, and A. Kot (2024). “Purify Unlearnable Examples via Rate-Constrained Variational Autoencoders”. In: *Forty-first International Conference on Machine Learning*.
- Yuan, C.-H. and S.-H. Wu (2021). “Neural Tangent Generalization Attacks”. In: *International Conference on Machine Learning*. PMLR, pp. 12230–12240.
- Zhang, J., X. Ma, Q. Yi, J. Sang, Y.-G. Jiang, Y. Wang, and C. Xu (2023). “Unlearnable clusters: Towards label-agnostic unlearnable examples”. In: *Proceedings of the IEEE/CVF Conference on Computer Vision and Pattern Recognition*, pp. 3984–3993.
- Zhou, L., A. Lou, S. Khanna, and S. Ermon (2024). “Denoising Diffusion Bridge Models”. In: *The Twelfth International Conference on Learning Representations*.
- Zhu, C., W. R. Huang, H. Li, G. Taylor, C. Studer, and T. Goldstein (2019). “Transferable clean-label poisoning attacks on deep neural nets”. In: *International Conference on Machine Learning*, pp. 7614–7623.
- Zhu, Y., L. Yu, and X.-S. Gao (2024). “Detection and defense of unlearnable examples”. In: *Proceedings of the AAAI Conference on Artificial Intelligence*. Vol. 38. 15, pp. 17211–17219.

A Data Protection and Data Poisoning Attacks

In this section, we formalize the relationship between data protection and data poisoning attacks. First, let us define data poisoning attacks: given a clean training set \mathcal{D}_c , data poisoning attacks create an additional poisoned set \mathcal{D}_p such that a model trained on $\mathcal{D}_c \cup \mathcal{D}_p$ exhibits behavior aligned with the adversary’s objective. These attacks can be categorized as: availability (or indiscriminate) attacks (e.g., Biggio et al., 2012; Koh and Liang, 2017; Koh et al., 2022; Muñoz-González et al., 2017; Lu et al., 2022; Suya et al., 2021; Lu et al., 2023; Lu et al., 2024) that reduce overall test performance, targeted attacks (e.g., Shafahi et al., 2018; Aghakhani et al., 2021; Guo and Liu, 2020; Zhu et al., 2019; Geiping et al., 2021), or backdoor attacks (e.g., Gu et al., 2017; Tran et al., 2018; Chen et al., 2017; Saha et al., 2020) that compromise model integrity for specific test samples or trigger patterns.

Data protection can be viewed as a special case of availability attacks where: (1) $|\mathcal{D}_c| = 0$, (2) \mathcal{D}_p is the protected dataset \mathcal{D}' , and (3) the adversary role is taken by the data protection service provider.

Finally, the inadequacy of data poisoning as a protection mechanism has been conclusively demonstrated, both through conceptual analysis (Radiya-Dixit et al., 2022) and technical evaluation (Hönig et al., 2024; Pooladzandi et al., 2024). Radiya-Dixit et al. (2022) identify a fundamental limitation in data protection methods: their “once for all” deployment mechanism fails to protect historical data and lacks cross-model transferability. While recent advances in transferable availability attacks (He et al., 2023; Ren et al., 2023; Wang et al., 2024) have partially addressed the model transferability challenge, our work reveals that the vulnerability of historical unprotected data (protection leakage) poses an even more significant security risk.

B Experiment Settings

B.1 Datasets

CIFAR-10/100. For CIFAR-10 and CIFAR-100 (Krizhevsky et al., 2012), the training set is divided into two parts: a set to be protected which contains 40,000 images, and a reference set comprising the remaining data. The images are 32×32 pixels.

ImageNet-Subset. The ImageNet-100 dataset consists of 100 classes selected from the full ImageNet dataset (Deng et al., 2009). Following Huang et al. (2021), Fu et al. (2022), and Qin et al. (2023), we use a subset of ImageNet-100 containing 85,000 images. The test set includes 50,000 images, the set to be protected contains 25,000 images, and the reference set includes 10,000 images. Images in both the protection and reference sets are resized to 224×224 pixels. For test images, the shorter edge is resized to 256 pixels, followed by a center crop to 224×224 .

WebFace-Subset. The CASIA-WebFace dataset (Yi et al., 2014) contains 494,414 face images of 10,575 real identities. We select the top 100 identities with the most images, resulting in a dataset of 44,697 images. This dataset is split into three parts: a test set comprising 4518 images, a protection set with 25,000 images, and a reference set containing the remainder. The images are 112×112 pixels.

Pets and Cars. Pets (Parkhi et al., 2012) contains 37 categories of animals, in which the set to be protected includes 3680 images and the test set contains 3669 images. Cars (Krause et al., 2013) contains 197 categories of automobiles, in which the set to be protected includes 8144 images and the test set contains 8041 images.

Table 5 summarizes the information about the datasets used for classification tasks. We delay the details of data preparation for the style mimicry task to Appendix B.5.

B.2 Protection

For CIFAR-10/100, ImageNet-Subset, and WebFace-Subset, we generate the availability attacks on the combination of the protection set and reference set to simulate the exact protection mechanism. The

Table 5: Dataset details.

	Protection	Reference	Test	Categories	Balanced
CIFAR-10	40,000	10,000	10,000	10	✓
CIFAR-100	40,000	10,000	10,000	100	✓
ImageNet-Subset	25,000	10,000	50,000	100	✓
WebFace-Subset	25,000	15,179	4,518	100	✗
Cars	8144	-	8041	197	✓
Pets	3680	-	3669	37	✓

additional paired data are collected from the original and protected reference datasets. In Appendix C.8, we will investigate more protections whose generation does not involve a reference dataset and present additional results showing the consistent effectiveness of BridgePure against them.

For Cars and Pets, the protection generation of UC(-CLIP) is determined by the clustering of the protection dataset. The generated protection can be easily applied to unseen data. Thus, we collect additional paired data from the protected test dataset.

For style mimicry protection, we will detail the implementation of Glaze and Mist in Appendix B.5.

B.3 BridgePure

Training. We train BridgePure from scratch using each paired dataset for 100,000 steps. The batch size is 32 for CIFAR-10, CIFAR-100, and WebFace-Subset; 16 for ImageNet-Subset; and 4 for *@nulevoy*'s artwork. Training on CIFAR-10/100 and WebFace-Subset can run on a single NVIDIA L40S/RTX 6000 Ada GPU with 40 GB memory. Training on ImageNet-Subset can run on a single NVIDIA A100 GPU with 80 GB memory. Training on artwork can run on 4 NVIDIA A100 GPUs in parallel. By default, we use the VE mode for bridge models and will compare VE and VP modes in Appendix C.7.

Sampling. We adopt 40-step sampling for all evaluated datasets. As recommended by DDBM (Zhou et al., 2024), the guidance hyper-parameter is set to 1 for VP bridge models and to 0.5 for VE bridge models.

B.4 Evaluation for Classification

To evaluate the restoration of availability, we train classifiers on the original/protected/purified datasets (i.e., protection set in Table 5) and calculate its accuracy on the test set. If not otherwise stated, we train a ResNet-18 classifier for 120 epochs using an SGD optimizer with an initial learning rate of 0.1, a momentum of 0.9, and a weight decay of 0.0005. The learning rate decays by 0.1 at the 80-th and 100-th epochs. The batch size is 128. For ViT and CaiT, we use Adam optimizer with an initial learning rate of 0.0005. We follow the evaluation setting from Zhang et al. (2023) for UC and UC-CLIP.

For contrastive learning, we train an encoder with the ResNet-18 backbone using SimCLR with a temperature of 0.5. The batch size is 512. We use an SGD optimizer with an initial learning rate of 0.5, a momentum of 0.9, and a weight decay of 0.0001. The learning rate scheduler is cosine annealing with a 10-epoch warm-up. The linear probing stage uses an SGD optimizer for 100 epochs with an initial learning rate of 1.0 and a scheduler that decays 0.2 at 60, 75, and 90-th epochs.

B.5 Style Mimicry

Artwork. After obtaining the artist's permission via email, we collect *@nulevoy*'s artwork from his homepage on *ArtStation*. The paintings are 1920×1080 pixels. Since Hönig et al. (2024) verified that Stable Diffusion v2.1 without fine-tuning fails to generate paintings of *@nulevoy*'s style, it is reasonable to use these artwork for the style mimicry task.

Protections. Glaze v2.1 takes an image of any shape as input and outputs a modified image of the same shape. Since it is a closed-source tool that only supports Windows and MacOS platforms, we process the paintings on a MacBook Pro with an M3 Max chip. The protected paintings have the same shape as the original ones. The protection intensity is *High* and the render quality is *Slowest*.

Mist takes square images and outputs images of the same shape. However, the max size it supports is 768×768 . To preserve the object ratios in the painting and the image quality, we first resize the short edge of images to 768, center-crop them to square ones, and then feed them into Mist. The resulting protected paintings are 768×768 pixels.

Mimicry pipeline. We adopt the style mimicry implementation from Hönig et al. (2024), which involves fine-tuning Stable Diffusion v2.1 (Rombach et al., 2022) using a set of captioned paintings. For fine-tuning, the images are first center-cropped to 512×512 and their captions are auto-generated by a BLIP-2 model (Li et al., 2023). The fine-tuned model generates 768×768 -pixel images based on predefined test prompts.

We randomly select 20 paintings from artist *@nulevoy* for fine-tuning and use the same 10 prompts⁵ from Hönig et al. (2024) to evaluate the mimicry performance. For Mist, the mimicry process performs center-cropping on the 768×768 squared images, while for Glaze, mimicry performs center-cropping on the original images.

BridgePure implementation. Assume a protection leakage consists of 5 or 10 pairs of original and protected artwork. To augment this dataset, we randomly crop the artwork to 512×512 pixels, generating a paired dataset with 1,000 pairs of paintings. BridgePure is then trained using this augmented paired dataset.

For the style mimicry task, the protected fine-tuning set comprises 20 paintings, which are center-cropped to 512×512 pixels from the protected outputs of Glaze or Mist. BridgePure sanitizes these images, and the purified outputs are subsequently fed into the mimicry pipeline.

C Additional Experiment Results

C.1 Visualization of Sanitized Images

We show original, protected, and BridgePure-purified images from CIFAR-10 and WebFace-Subset in Figure 9. Although availability attacks make perturbations less noticeable by imposing norm constraints, upon zooming in and comparing the protected image with the original, one can observe slight differences. However, images purified by BridgePure are indistinguishable from the original to human eyes.

Figure 10 provides additional generated images in the style mimicry task investigated by Section 5.3. As discussed in Section 5.3, BridgePure eliminates the protective cloaks in the mimicry outputs.

C.2 Time Consumption

On our machine with NVIDIA A100 GPUs, training a BridgePure on CIFAR-10/100 costs around 22.5 hours with a single GPU, and that on ImageNet-Subset costs around 24 hours with a single GPU. For sampling a batch of 64 images from ImageNet-Subset with a single GPU, BridgePure costs 138 seconds on average while DiffPure ($t^*=0.1$) costs 165 seconds.

C.3 Minor Protection Leakage

In previous tables, we report the results of BridgePure trained with protection leakage ranging from 500 to 4000 pairs. Figure 11 investigates the performance of BridgePure with less leakage, i.e., from 20 to 500 pairs, on CIFAR-10 and CIFAR-100 protected by LSP. For CIFAR-10, 100 pairs are sufficient for BridgePure to

⁵The prompts for style mimicry include “a mountain by nulevoy”, “a piano by nulevoy”, “a shoe by nulevoy”, “a candle by nulevoy”, “a astronaut riding a horse by nulevoy”, “a shoe with a plant growing inside by nulevoy”, “a feathered car by nulevoy”, “a golden apple by nulevoy”, “a castle in the jungle by nulevoy”, and “a village in a thunderstorm by nulevoy”.

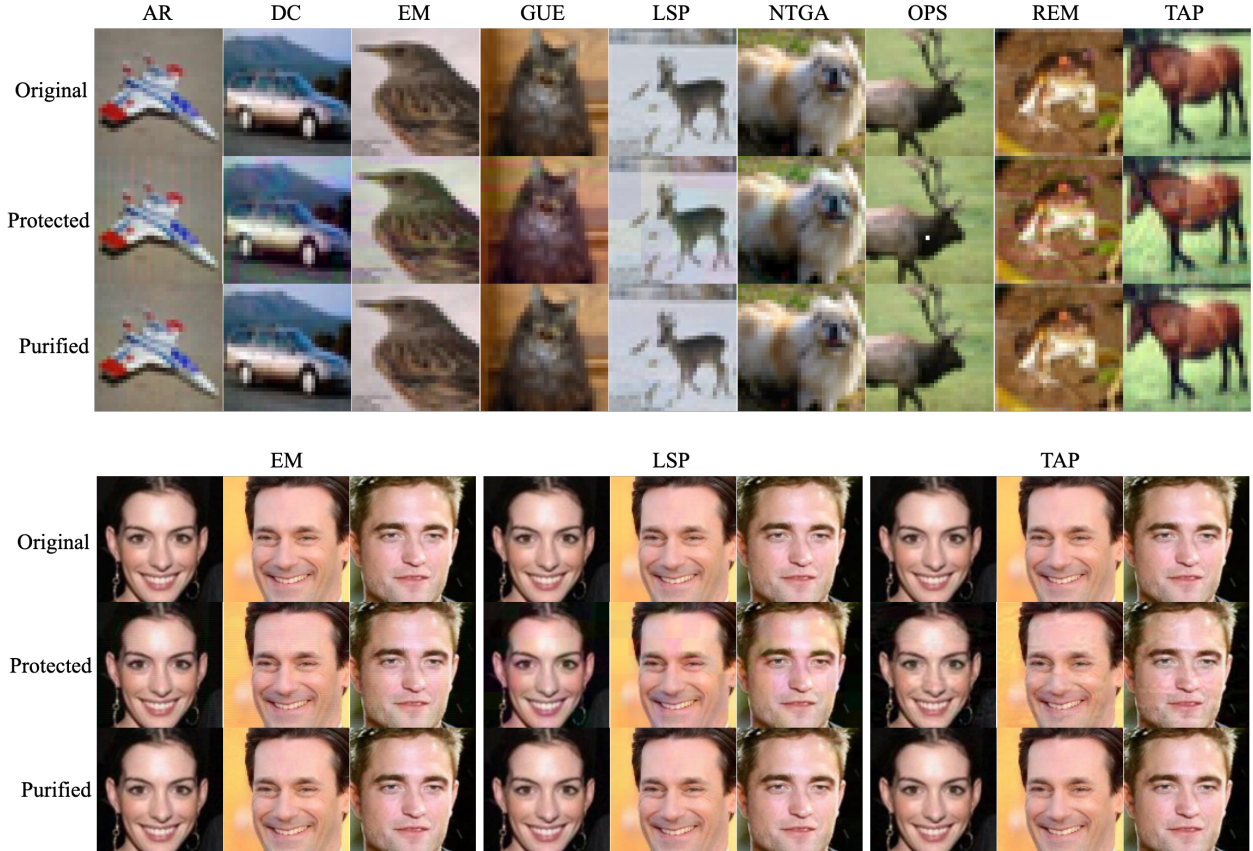


Figure 9: Visualization of our BridgePure-1K on CIFAR-10 (**top**) and WebFace-Subset (**bottom**).

improve the test accuracy to 93%, while for CIFAR-100, BridgePure-100 only restores the accuracy to 50% and BridgePure-200 improves it to 69%. This difference in purification performance with minor protection leakage is because CIFAR-100 has 10 times more categories and thus the leakage in each class is much less than that for CIFAR-10.

C.4 Evaluation with More Networks Architectures

In Table 6, we evaluate the purified CIFAR-10 datasets for classification using various network architectures, including SENet-18 (Hu et al., 2018), MobileNet v2 (Sandler et al., 2018), DenseNet-121 (Huang et al., 2017), ViT (Dosovitskiy et al., 2021), and CaiT (Touvron et al., 2021). It shows that the purification effect of BridgePure is consistent across networks.

Table 6: We evaluate BridgePure-1K-sanitized CIFAR-10 datasets using different network architectures. The baseline is trained on unprotected data.

	Baseline	AR	DC	EM	GUE	LSP	NTGA	OPS	REM	TAP
SENet-18	94.00 \pm 0.18	91.79 \pm 0.26	93.78 \pm 0.12	93.73 \pm 0.11	93.77 \pm 0.31	93.96 \pm 0.15	93.96 \pm 0.18	93.28 \pm 0.16	92.32 \pm 0.36	87.37 \pm 0.10
MobileNet v2	90.60 \pm 0.29	87.63 \pm 0.44	90.29 \pm 0.11	90.17 \pm 0.18	90.40 \pm 0.10	90.43 \pm 0.15	90.73 \pm 0.42	90.32 \pm 0.12	89.03 \pm 0.38	84.54 \pm 0.24
DenseNet-121	94.44 \pm 0.15	92.24 \pm 0.16	94.32 \pm 0.23	93.92 \pm 0.29	94.11 \pm 0.14	94.07 \pm 0.16	94.37 \pm 0.10	93.74 \pm 0.12	92.93 \pm 0.24	87.75 \pm 0.26
ViT	84.80 \pm 0.15	84.61 \pm 0.27	84.48 \pm 0.50	84.26 \pm 0.11	83.94 \pm 0.52	84.80 \pm 0.39	84.82 \pm 0.21	84.89 \pm 0.43	83.95 \pm 0.08	80.05 \pm 0.34
CaiT	82.73 \pm 0.23	82.53 \pm 0.18	82.20 \pm 0.78	81.91 \pm 0.45	81.58 \pm 0.43	82.55 \pm 0.21	82.71 \pm 0.15	82.41 \pm 0.25	81.90 \pm 0.15	78.09 \pm 0.33

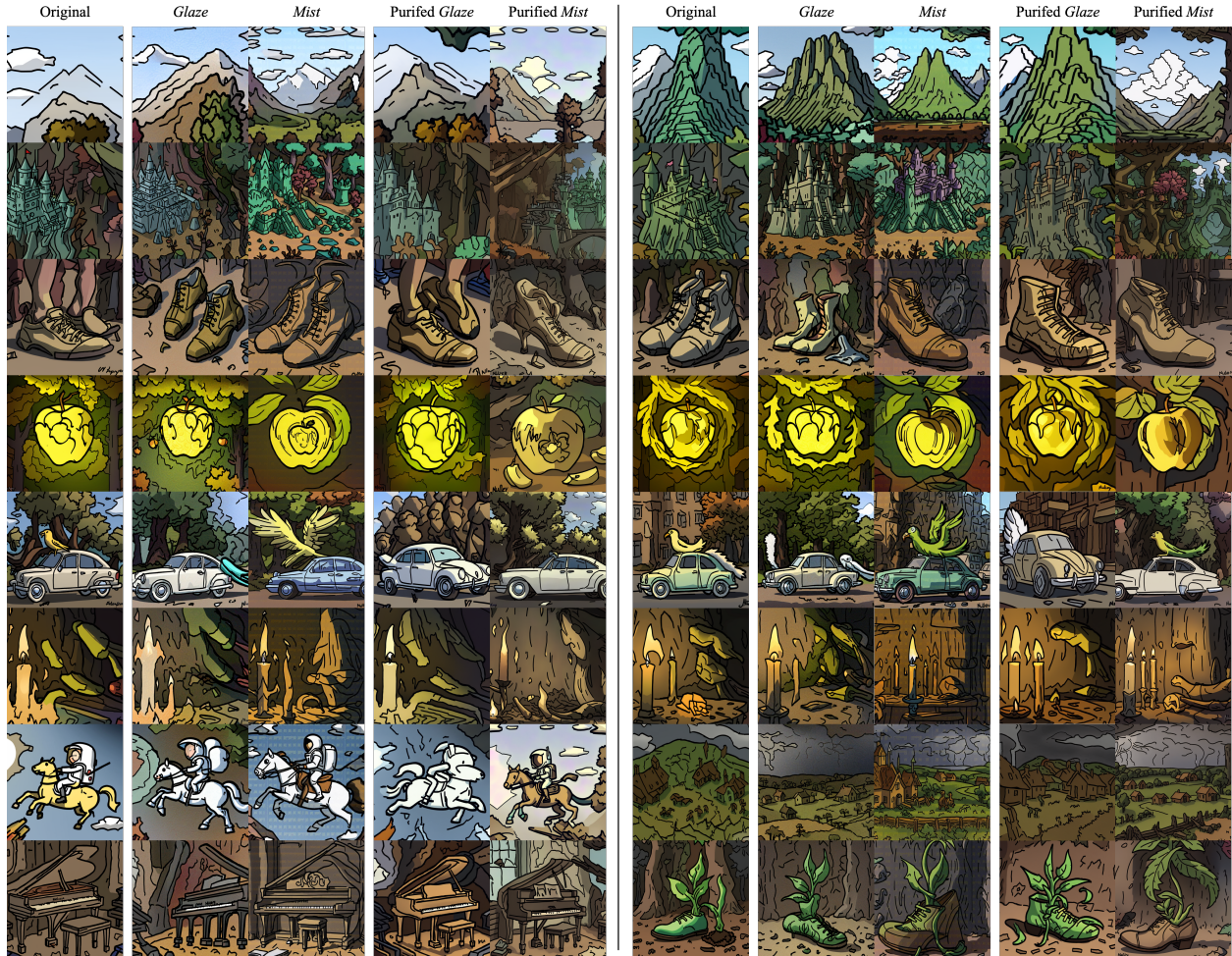


Figure 10: Additional results to Figure 7. Performance of BridgePure-5 (left) and BridgePure-10 (right) for style mimicry.

C.5 Transferability across Protections

We consider a scenario in which the adversary collects some additional data \mathcal{D}_a but calls a different protection mechanism from \mathcal{P} that protects \mathcal{D} , and then derives a BridgePure using such pairs. In this case, the purification ability of BridgePure reflects its transferability across different protections. Figure 12 shows BridgePure has limited transferability across protections and advanced purification relies on the awareness of the underlying mechanism for the protected data.

C.6 Transferability across Data Distributions.

In our threat model, we assume the additional dataset \mathcal{D}_a is sampled from the same distribution as that for \mathcal{D} . Now we consider a scenario where an adversary cannot collect additional data from the exact same distribution but from a similar distribution, e.g., \mathcal{D} is from CIFAR-10 and \mathcal{D}_a is from CIFAR-100, or vice versa. We investigate the influence of such distribution mismatch on the purification performance of BridgePure in Table 7. When BridgePure is trained on pairs from CIFAR-100 and is used to purify protected images from CIFAR-10, the accuracy for OPS and LSP is over 90% but that for other protections is lower than 80%. When BridgePure is trained on pairs from CIFAR-10 and is used to purify protected images from CIFAR-100,

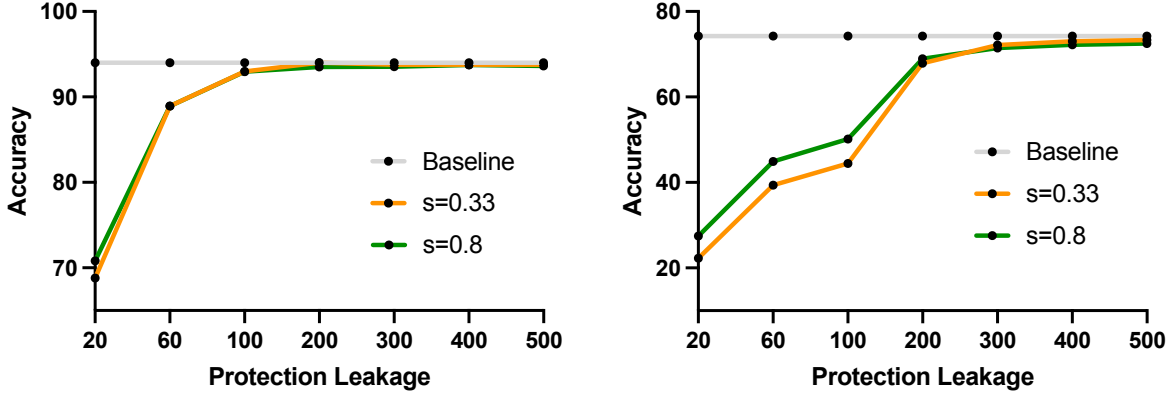


Figure 11: Purification performance of BridgePure with small protection leakages to purify LSP-protected CIFAR-10 (left) and CIFAR-100 (right). Here $\beta = 0$ and $s \in \{0.33, 0.8\}$.

the accuracy for all the nine protections is lower than 60%. The reasons why BidgePure transfers well from CIFAR-100 to CIFAR-10 for LSP and OPS could be (1) OPS and LSP create rather regular patterns for protection while other methods generate irregular patterns (see Figure 9); (2) CIFAR-100 is more fine-grained than CIFAR-10 and thus CIFAR-100 pairs might cover the protection mechanism for CIFAR-10.

Table 7: Transferability of BridgePure-4K across CIFAR-10 and CIFAR-100. For example, CIFAR-100 \rightarrow CIFAR-10 means BridgePure is trained using protection leakage of CIFAR-100 and is used to purify protected CIFAR-10. Here $s = 0.33$ and $\beta = 0$.

Transfer		AR	DC	EM	GUE	LSP	NTGA	OPS	REM	TAP
CIFAR-100 \rightarrow CIFAR-10 (94.01 \pm 0.15)	Protected	13.52 \pm 0.63	15.10 \pm 0.81	23.79 \pm 0.13	12.76 \pm 0.44	13.85 \pm 0.96	12.87 \pm 0.23	13.67 \pm 1.80	20.96 \pm 1.70	9.51 \pm 0.67
	Purified	32.16 \pm 0.36	37.33 \pm 3.05	63.90 \pm 0.80	27.65 \pm 0.73	90.26 \pm 0.26	65.94 \pm 1.02	93.43 \pm 0.27	30.22 \pm 0.78	78.18 \pm 0.55
CIFAR-10 \rightarrow CIFAR-100 (74.27 \pm 0.45)	Protected	2.02 \pm 0.12	36.10 \pm 0.67	6.73 \pm 0.12	19.50 \pm 0.48	2.56 \pm 0.16	1.51 \pm 0.22	12.18 \pm 0.52	7.07 \pm 0.19	3.59 \pm 0.12
	Purified	13.74 \pm 0.26	53.22 \pm 0.78	42.96 \pm 0.50	33.55 \pm 0.62	54.33 \pm 0.93	28.91 \pm 1.53	58.18 \pm 1.74	15.89 \pm 0.14	41.75 \pm 0.32

C.7 Comparison between VE and VP Bridges

DDBM (Zhou et al., 2024) supports two modes for the diffusion process: variance exploding (VE) and variance preserving (VP). Figure 13 compares the performance of VE and VP bridges on CIFAR-10 and CIFAR-100. When facing REM and TAP attacks on CIFAR-100, the VE bridge consistently outperforms the VP bridge for two values of s . In other cases, the purification effects of the two modes are comparable. Therefore, we adopt the VE bridge as the default setting in this paper.

Table 8: Purification performance on CIFAR-10 and CIFAR-100 against EMC*, OPS* and TAP* protections.

	EMC*	OPS*	TAP*	EMC*	OPS*	TAP*
	CIFAR-10 (94.01 \pm 0.15)			CIFAR-100 (74.27 \pm 0.45)		
Protected	13.05 \pm 0.54	12.01 \pm 0.97	7.68 \pm 0.50	1.41 \pm 0.11	12.44 \pm 0.66	3.24 \pm 0.32
BridgePure-0.5K	93.98 \pm 0.17	92.99 \pm 0.02	80.20 \pm 0.28	74.46 \pm 0.16	73.70 \pm 0.14	59.31 \pm 0.38
BridgePure-1K	94.06 \pm 0.10	93.52 \pm 0.30	82.44 \pm 0.40	74.54 \pm 0.17	74.26 \pm 0.16	63.79 \pm 0.29
BridgePure-2K	93.85 \pm 0.17	93.14 \pm 0.23	90.55 \pm 0.23	74.22 \pm 0.39	74.38 \pm 0.25	63.01 \pm 0.56
BridgePure-4K	93.95 \pm 0.15	93.92 \pm 0.08	93.07 \pm 0.19	74.00 \pm 0.39	74.36 \pm 0.38	69.92 \pm 0.13

AR	80.0	5.0	-1.0	-2.1	-1.6	-0.5	-0.4	11.1	24.0
DC	0.4	78.7	40.3	7.9	-0.6	11.6	0.7	5.3	13.6
EM	0.3	16.0	70.1	-0.1	0.2	1.2	-0.1	10.0	1.3
GUE	0.8	24.7	10.9	81.1	0.2	1.3	0.4	34.0	-0.1
LSP	3.8	42.5	20.0	10.1	80.1	27.4	2.8	15.9	15.6
NTGA	8.4	46.8	37.4	1.7	4.5	81.1	4.8	44.1	36.6
OPS	0.1	0.2	0.8	1.4	-0.6	1.5	79.8	-0.8	2.2
REM	0.2	2.1	4.5	-0.1	2.4	2.1	-0.5	72.5	3.3
TAP	-0.4	3.1	0.0	0.8	0.0	0.7	-0.5	2.3	83.4

Figure 12: Transferability of BridgePure-4K across different protections on CIFAR-10. The **x-axis** represents the protection leakage on which BridgePure is trained. The **y-axis** represents the protected dataset to which the pre-trained BridgePure is applied for purification. Each cell shows an improvement in test accuracy compared to the unpurified dataset. Here $s = 0.33$ and $\beta = 0$.

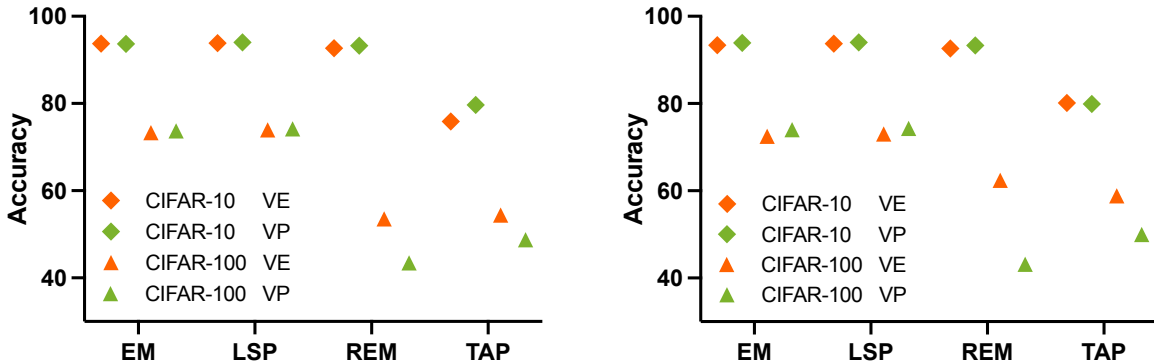


Figure 13: Comparison between VP and VE modes of BridgePure-1K with $s = 0.33$ (left) and with $s = 0.8$ (right). Here $\beta = 0$.

C.8 More Discussion on Protection for Additional Data

Note that our threat model assumes that the protection mechanism \mathcal{P} can generate (unprotected, protected) pairs using only the additional data \mathcal{D}_a . While some availability attacks such as LSP, UC, UC-CLIP, Glaze, and Mist are precisely examined in this way, some other attacks may not fit exactly into the threat model. For example, EM and REM generate sample-wise protection on the dataset they optimize. Thus performing the protections on \mathcal{D} and \mathcal{D}_a separately may result in different protection mechanisms.

To ensure that the protection is consistent for \mathcal{D} and \mathcal{D}_a , we generate the protection using both \mathcal{D} and the reference set from which \mathcal{D}_a is sampled and evaluate the attacks in Tables 1 and 2. This may pose a slightly stronger protection leakage that allows an adversary to directly obtain the additional pairs. Here we consider three additional variants of the attacks we considered previously and allow access to \mathcal{D}_a only:

- EMC*: We generate class-wise EM protection (Huang et al., 2021) using the 40K images to be protected

and apply the protection to additionally collected data.

- OPS*: Similar to EMC*, we generate OPS protection (Wu et al., 2023) using the 40K images to be protected and apply the protection to additionally collected data.
- TAP*: The reference classifier is trained on the 40K images, and the protection for additional data is to search adversarial examples for this classifier (Fowl et al., 2021).

We evaluate these three protections on CIFAR-10 and CIFAR-100 in Table 8 and the results confirm the potent purification ability of BridgePure that is consistent with the previous results in Section 5.2.